AIR ENTRAINMENT IN ANGLED DIP COATING

Olivier Cohu and Hadj Benkreira[1]

Department of Chemical Engineering, University of Bradford
West Yorkshire, BD7 1DP, United Kingdom

ABSTRACT

The coating flow examined here, labelled angled dip coating, is that where a substrate enters a pool of liquid forming an angle β with the vertical so that it intersects the liquid along a wetting line which is not perpendicular to the direction of its motion. This flow situation is distinctly different from that where the substrate, inclined in the other dimension by the so-called angle of entry α, intersects the liquid surface perpendicularly to its motion. Experiments were carried out with various liquids to determine the effect of β on the substrate velocity at which air is entrained into the liquid. It was observed that as this angle departs from zero, air entrainment is delayed to higher speeds. The data show that the speed which is relevant to air entrainment is not the velocity of the substrate itself but its component normal to the wetting line. This result has important practical implications and suggests that this fundamental principle is also applicable to other coating flows.

Keywords : *Dip Coating - Coating flows - Air entrainment - Dynamic wetting - Contact angle - Experiments*

1. INTRODUCTION

The principle of all coating operations is that air in contact with a dry solid substrate is displaced by a liquid film. At low substrate speeds a uniform film is formed but as the speed increases, air is entrained between the coating and the solid and spoils the quality of the coating which becomes mared with bubbles. When the coating dries, these bubbles leave defects on the final coated product which becomes wasted. This phenomenon is observed in all coating processes and is one of the most serious limitation to coating operations where high throughput and absolute uniformity are required.

The study of air entrainment in coating flows has largely been based on dip coating experiments where a smooth flat substrate is plunged into a large pool of stagnant liquid, a simple flow situation which attempts to extract the essence of the problem at the three phase, solid / liquid / gas contact line in more complex coating flows. Such a flow reveals that the free surface of the liquid intersects the solid substrate along the *wetting line* and forms with it the *dynamic contact angle* measured through the liquid

[1] corresponding author : Tel (01274) 383721 Fax (01274) 385700 Email H.Benkreira@bradford.ac.uk

as shown in fig. 1. As the speed of the substrate is increased, the wetting line moves downward and the contact angle increases until it approaches 180° at the critical velocity $V_{ae.}$ Detailed descriptions of the mechanism of air entrainment have been given by O'Connell (1989), Burley (1992), and Veverka (1995), but Deryagin and Levi (1964) noted first that when the critical velocity is reached, the dynamic wetting line which is originally straight and horizontal becomes unsteady and breaks into straight-line segments that are inclined from the horizontal. At any instant, the wetting line has an appearance of sawteeth (fig. 2), and air is entrained at the trailing vertices where two straight-line segments seem to intersect. This phenomenon is termed *gross air entrainment* to contrast it with the *microscopic regime of air entrainment* which was observed by Miyamoto and Scriven (1982) and Miyamoto (1991) at speeds lower than V_{ae}. Gross air entrainment only will be considered in this paper.

Many attempts have been made to correlate the critical velocity V_{ae} with the properties of the fluid and the substrate involved. Buonoplane *et al.*(1986) concluded from their experiments that substrate roughness leads to higher critical velocities, as was inferred previously by Scriven (1982). They also showed that surface wettability has little or no effect. Using smooth substrates, Burley and Kennedy (1976) derived the following empirical correlation,

$$V_{ae} \approx 67.7 \left[\mu \left(\frac{g}{\rho\sigma} \right)^{0.5} \right]^{-0.67} \qquad [1]$$

whereas Burley and Jolly (1984) obtained

$$V_{ae} \approx 70.5 \left[\mu \left(\frac{g}{\rho\sigma} \right)^{0.5} \right]^{-0.77} \qquad [2]$$

Here g is the gravity constant, and μ, σ, and ρ are the viscosity, the surface tension and the density of the liquid, respectively. Being dimensionally inconsistent, both eqs. [1] and [2] are written here in c.g.s. units. Dimensionless correlations were also given, but the lack of readily accessible characteristic length weakens their practical interest.

Gutoff and Kendrick (1982) found experimentally that viscosity was the sole relevant parameter, and then proposed the correlation

$$V_{ae} \approx 5.11\, \mu^{-0.67} \qquad [3]$$

in which V_{ae} is expressed in cm/s and μ in mPa.s. Their data were in good agreement with eqs. [1] and [2] as both surface tension and density are second order parameters and are unlikely to vary significantly in practical situations.

Blake and Ruschak (1979) observed the geometry of the sawteeth shaped wetting line at speeds higher than V_{ae} and established that the component of the speed normal to

the straight-line segments of the wetting line was independent of the substrate velocity. They termed this component, the *maximum speed of wetting,* V* which they assumed is the maximum speed at which the wetting line can advance normal to itself. They observed that the substrate could be wet at speeds V higher than V* only if the wetting line slanted so that the speed of the solid normal to it did not exceed the maximum speed of wetting. More specifically, they found that the wetting line segments adopted the minimum possible inclination Φ such that

$$\cos \Phi = V^*/ V \qquad (V \geq V^*), \qquad [4]$$

see fig. 2. This would explain the break-up of the wetting line into a sawteeth pattern and the subsequent occurrence of air entrainment at the point where two straight-line segments seem to intersect. The observation of a maximum speed at which a three-phase contact line can advance normal to itself has been also reported by Petrov and Sedev (1985) who investigated the similar phenomenon of dewetting. Theoretical support of these observations has been given later by Blake (1993) and Shikhmurzaev (1993).

Blake and Ruschak (1979) pointed out that the existence of a maximum speed of wetting would imply that the break-up of the wetting line, hence the occurrence of air entrainment could be postponed to velocities V_{ae} greater than V* provided that the substrate does not enter the bath *vertically*. They claimed to have observed this experimentally but surprisingly did not substantiate this important argument with experimental data. Since then, the possible influence of the angle at which the solid plunges into the liquid has been much debated. Burley and Jolly (1984) found that the critical velocities did not change with the *angle of entry*, although they could observe slight differences between the two sides of the tape. They concluded that Blake and Ruschak's (1979) analysis was incorrect (Burley, 1992). However, they did not realise that they had considered the effect of a *different* angle (α in fig. 3a). In their set-up, the substrate, though inclined, intersected the fluid perpendicularly to its motion (fig. 3a) whereas in the arrangement of Blake and Ruschak (1979) the substrate must be inclined at an angle β in another dimension, so that the wetting line is not perpendicular to the direction of substrate motion, as depicted in fig. 3b. The same error was made by Ghannam and Esmail (1990) who studied the case of a rotating cylinder partially immersed in a liquid pool. They could vary the angle of *entry* by raising or lowering the roller axis. Contrary to Burley and Jolly (1984), they found the air entrainment velocity to depend significantly on the angle of entry, and mistakenly concluded that their results were in agreement with the predictions of Blake and Ruschak (1979). So far then, the simple yet fundamental effect of having the angle formed by the wetting line and the substrate velocity vector different from 90° (fig. 3b) has not been tested experimentally comprehensively and conclusively. This is precisely the aim of this paper.

2. EXPERIMENTAL SET-UP

The experimental apparatus is depicted schematically in fig. 4. A 50 mm wide polypropylene tape was drawn downwards through a perpex tank containing the liquid. The tape passed over grounded metal rollers to reduce any static charges

(Burley and Jolly, 1984), plunged into the liquid, emerged from a narrow slit at the bottom of the tank and was finally wound around a cylinder driven by a variable speed motor. This design prevented the fluid carried along the substrate from flowing back and entraining air bubbles into the tank. Additional liquid was supplied regularly to the tank to compensate for the amount entrained out of the pool by the substrate.

The whole system, including the tank and the motor, was rather compact, the inter-axes distance between the feed reel and the take-up reel being approximately 55 cm. It was mounted on a stainless steel frame that could pivot sideways. While remaining is the vertical plane, the tape could be inclined laterally up to 55° from the vertical by increments of 5°. The height of the tank ensured that the depth of the liquid was at least 5 cm even at the maximum inclined angle.

Three glycerine-water solutions and one vegetable oil were used as Newtonian test fluids. Their viscosities were measured to an accuracy of ± 5% with a Brabender Rheotron rheometer equipped with a Couette geometry. Surface tensions were measured to within ± 2 % using the pendent drop method. The physical properties of the liquid used are listed in table 1.

The tape velocities were measured with an optically triggered digital tachometer mounted on one of the rollers. All the experiments were conducted at room temperature, that is between 20 and 25°C. The physical properties of the liquids were measured at the temperature recorded during the coating experiments, which did not vary significantly during the processing of each individual liquid.

3. DETERMINATION OF THE ONSET OF AIR ENTRAINMENT

The onset of air entrainment was determined by slowly increasing the tape velocity until the break-up of the wetting line into a sawteeth pattern could be observed. The speed reached was then recorded as the onset of air entrainment. Whether or not visible air bubbles were actually dragged into the liquid from the tip of the v-shapes was not considered. The reason is that the entrainment of air bubbles into the liquid is much more difficult to detect than the break-up of the wetting line, which could be easily observed with the naked eye under proper illumination. It was therefore assumed that the break-up of the wetting line and the onset of air entrainment were confounded, which may be not rigorously the case in practise (Burley, 1992 ; Veverka and Aidun, 1997). In order to reduce experimental errors, each data point was repeated at least four times. In spite of the relative crudeness of the experimental method, the discrepancies between individual and averaged data was always found to be less than ± 10%, being even less than ± 7% in most cases.

4. RESULTS AND DISCUSSION

4.1. Air entrainment velocity for a vertical tape

In order to validate the experimental technique, the experimental values of the onset of air entrainment obtained with a vertical tape ($\beta = 0$) were compared with the

predictions of Burley and Kennedy (1976), Burley and Jolly (1984), and Gutoff and Kendrick (1982). The results are shown in figs. 5 and 6. The correlation of Burley and Jolly (1984) fits our data best. The agreement with Gutoff and Kendrick's (1982) correlation, is less good, probably because both surface tension and density, which play a role albeit a minor one, do not enter in their correlation. It is worth noting that for the glycerine solutions n^{os} 2 and 3 of high densities and surface tensions, the air entrainment velocities are greater than predicted by Gutoff and Kendrick's correlation, whereas for the vegetable oil of low density and surface tension, the air entrainment velocity is lower than predicted. With the glycerine solution n^{o} 1, which has the highest viscosity, the observed air entrainment speed is in very good agreement with the prediction. This confirms that viscosity is the dominant parameter and that the air entrainment velocity increases with both density and surface tension.

4.2. Air entrainment velocity for a laterally inclined tape

With the four liquids tested, the air entrainment velocity was found to increase significantly as the tape axis departed from the vertical. For instance, the air entrainment velocity at $\beta = 55°$ was measured to be about 1.75 times that obtained for $\beta = 0$ (vertical tape). A typical result is shown in fig. 7 for glycerine solution n^{o} 2.

According to Blake and Ruschak (1979), the break-up of the wetting line should occur when the component of the tape velocity normal to the horizontal exceeds the maximum speed of wetting V*. The air entrainment velocity for a given angle β is then expected to verify

$$V_{ae} = V^*/\cos\beta \qquad [5]$$

where V* is the air entrainment velocity at $\beta = 0$. Eq. [5] can be rewritten in a dimensionless form as

$$V_{ae} \cos\beta / V^* = 1. \qquad [6]$$

The experimental data obtained for the four liquids used were tested against eq. [6]. The results are shown in fig. 8. Regardless of the liquid involved, it can be seen that the data follow the predictions of Blake and Ruschak (1979) fairly well, the scattering of the data being of same order as the experimental uncertainties (± 10%). This shows that the speed which is relevant in the dynamic wetting process is not the velocity of the substrate itself but its component normal to the wetting line.

Another evidence of this arises from the observation of the sawteeth shaped wetting line at speeds greater than V_{ae} and for $\beta \neq 0$. Not surprisingly, the triangular air pockets which were observed throughout the experiments were no longer symmetrical for $\beta \neq 0$. In full agreement with Blake and Ruschak (1979) indeed, they formed in such a way that both sides of the v-shapes formed the same angle with the substrate velocity vector (fig. 9). This confirms that the wetting line adopts a sawteeth pattern that prevents the component of the speed normal to it to exceed the maximum speed of wetting.

5. CONCLUDING REMARKS

This work has provided new experimental evidence of the existence, for a given solid / liquid / gas system, of a maximum speed of wetting understood as the maximum speed at which a dynamic wetting line can advance normal to itself in dip-coating experiments. As pointed out by Blake and Ruschak (1979), this could *explain* the break-up of the wetting line into a sawteeth pattern when the critical velocity is reached and the subsequent air entrainment at the tip of the v-shapes. However, it should be emphasised that our experiments do not give any insight on the *physical origin* of the maximum speed of wetting. Blake (1993) derived a molecular kinetic theory of dynamic wetting in which the maximum speed of wetting appears to be of non-hydrodynamic origin. On the other hand, high-speed visualisations of the contact line (Veverka, 1995) suggest that the formation of triangular air pockets at V_{ae} is actually of hydrodynamic origin (Veverka and Aidun, 1997). In addition, there are considerable evidence that the critical speed for air entrainment depends strongly on the flow field in the liquid phase (Perry, 1967 ; Blake *et al.*, 1994 ; Veverka, 1995). In our experiments, inclining the substrate with respect to the vertical altered not only the angle formed by the wetting line and the substrate velocity vector but also the air and liquid flow fields near the contact line. This could also explain the effect of substrate lateral inclination in delaying the onset of air entrainment.

The existence of a maximum speed of wetting as defined above implies that the speed which is relevant to air entrainment in coating operations is not the velocity of the substrate itself but its component normal to the wetting line. Using this fact, a simple and efficient way has been proposed to postpone the occurrence of air entrainment to higher substrate speeds. It is based on having the angle formed by the wetting line and the substrate velocity different from 90°. In dip coating, where a continuous dry tape enters a large pool of liquid, this was achieved by inclining the substrate laterally in the vertical plane. It has been shown experimentally that the air entrainment velocity is multiplied by the expected factor $1/\cos\beta$ when the tape is laterally inclined by an angle β from the vertical.

In practical terms, this means that a gain of about 75 % on the coating speed can be achieved by inclining the substrate laterally by an angle of 55° from the vertical, as was found experimentally. It is clear, however, that having the substrate inclined sideways would pose problems in industrial practise. Nevertheless, the principle of slanting the wetting line to delay the onset of air entrainment should be applicable more easily to pre-metered coating methods such as curtain coating and extrusion coating where this may be done by inclining the coating head instead of the substrate. Testing this idea and its consequences on the coating thickness and the stability of the flow is currently under investigation.

6. ACKNOWLEDGEMENTS

This work was supported by a grant awarded to Dr. O. Cohu under the Training and Mobility of Researchers Programme of the Commission of European Communities. The contribution of Dr. R. Patel and C. Mistry to the design of the experimental rig is

gratefully acknowledged. We would like to thank Professor C.K. Aidun for having provided us with a preprint of his paper.

7. NOTATIONS

V	Substrate speed
V^*	Maximum speed of wetting
V_{ae}	Air entrainment velocity
g	Gravity constant ($g \approx 9.81$ m.s^{-2})
α	Substrate entry angle
β	Substrate lateral inclination
Φ	Inclination of the wetting line at $V > V_{ae}$
μ	Viscosity
ρ	Density
σ	Surface tension

8. REFERENCES

Blake, T.D., "Dynamic Contact Angles and Wetting Kinetics", *in* "Wettability", J. Berg Ed., Marcel Dekker, New-York, Chap. 5, 252 (1993)

Blake, T.D., Clarke, A., and Ruschak, K.J., "Hydrodynamic Assist of Dynamic Wetting", *AIChE J.*, **40**, 229 (1994)

Blake, T.D. and Ruschak, K.J., "A Maximum Speed of Wetting", *Nature*, **282**, 489 (1979)

Buonoplane, R.A., Gutoff, E.B. and Rimore,M.M.T., "Effect of Plunging Tape Surface Properties on Air Entrainment Velocity", *AIChE J.*, **32**, 682 (1986)

Burley, R., "Air Entrainment and the Limits of Coatability", *JOCCA*, **75**(5), 192 (1992)

Burley, R. and Jolly, R.P.S., "Entrainment of Air into Liquids by a High Speed Continuous Solid Surface", *Chem. Eng. Sci.*, **39**, 1357 (1984)

Burley, R. and Kennedy, B.S., "An Experimental Study of Air Entrainment at a Solid-Liquid-Gas Interface", *Chem. Eng. Sci.*, **31**, 901 (1976)

Deryagin, B.M., and Levi, S.M., "Film Coating Theory", Focal Press, London, 137 (1964)

Ghannam, M.T. and Esmail, M.N., "Effect of Substrate Entry Angle on Air Entrainment in Liquid Coating", *AIChE J.*, **36**, 1283 (1990)

Gutoff, E.B. and Kendrick, C.E., "Dynamic Contact Angles", *AIChE J.*, **28**, 459 (1982)

Miyamoto, K., “On the Mechanism of Air Entrainment”, *Ind. Coat. Res.*, **1**, 71 (1991)

Miyamoto, K. and Scriven, L.E., “Breakdown of Air Film Entrained by Liquid Coated on a Web”, *AIChE Annual Meeting, Los Angeles, CA* (1982)

O'Connell, A., “Observation of Air Entrainment and the Limits of Coatability”, PhD Thesis, Heriot-Watt University, Edinburgh, Scotland (1989)

Perry, R.T., “Fluid Mechanics of Entrainment through Liquid-Liquid and Liquid-Solid Junctures”, PhD Thesis, University of Minnesota (1967)

Petrov, J.G. and Sedev, R.V., “On the Existence of a Maximum Speed of Wetting”, *Coll. Surf.*, **13**, 313 (1985)

Scriven, L.E., “How Does Air Entrain at Wetting Lines”, *AIChE Winter Nat. Meet., Orlando, FL.* (1982)

Shikhmurzaev, Y.D., “The Moving Contact Line on a Smooth Solid Surface”, *Int. J. Multiphase Flow*", **19**, 589 (1993)

Veverka, P.J., “An Investigation of Interfacial Instability during Air Entrainment”, PhD Thesis, Institute of Paper Science and Technology, Atlanta, GA. (1995)

Veverka, P.J. and Aidun, C.K., “Dynamics of Air Entrainment at the Contact Line”, *submitted to J. Fluid Mech.* (1997)

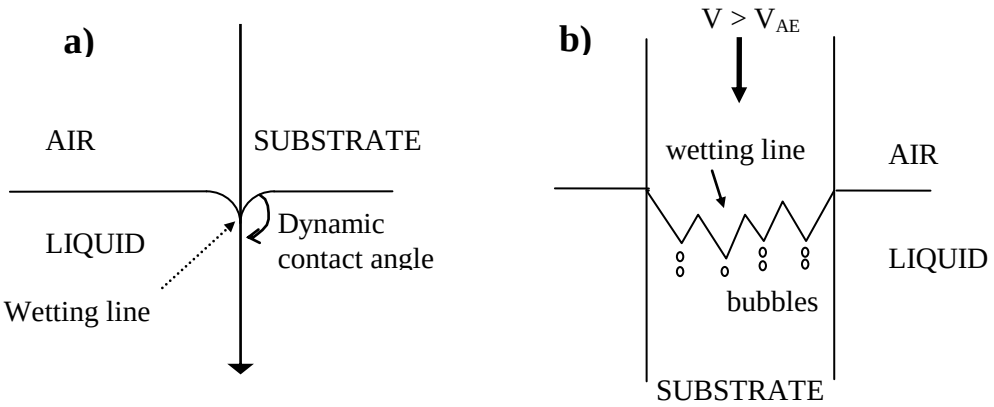

Fig. 2 : Dynamic wetting features in plunging tape experiments, a) dynamic contact angle, b) break-up of the wetting line and air entrainment at speeds higher than V_{AE}

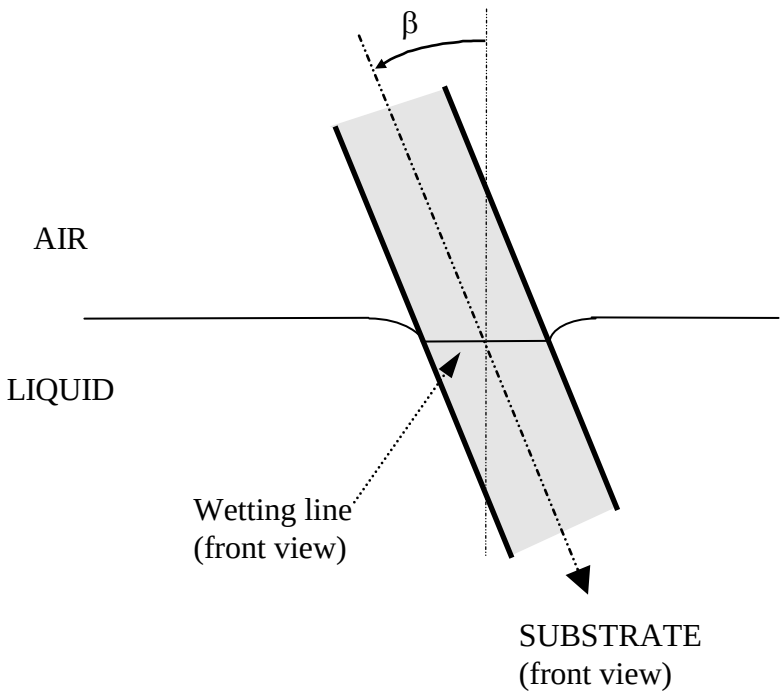

Fig. 3 : Angled dip-coating configuration studied by Cohu and Benkreira (1997)

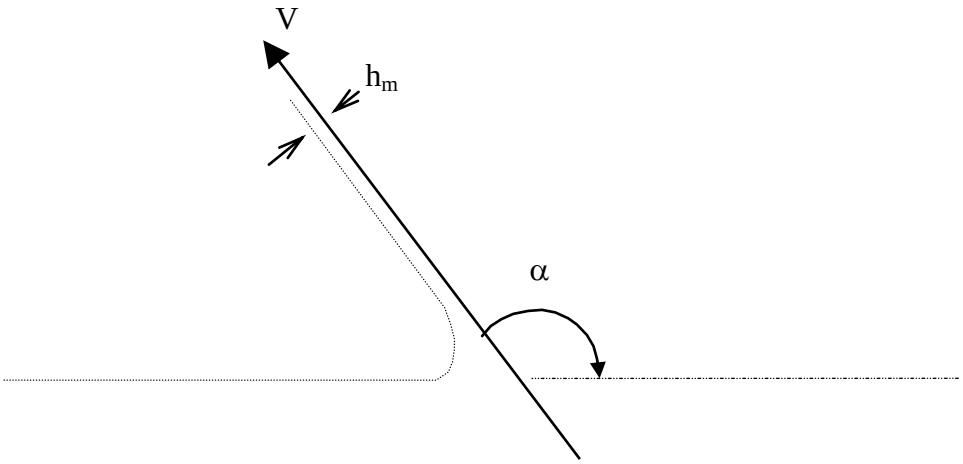

Fig. 4 : Free coating flow

Fig. 5 : Variation of dimensionless film thickness with capillary number in dip-coating (after Schunk *et al.* 1997)

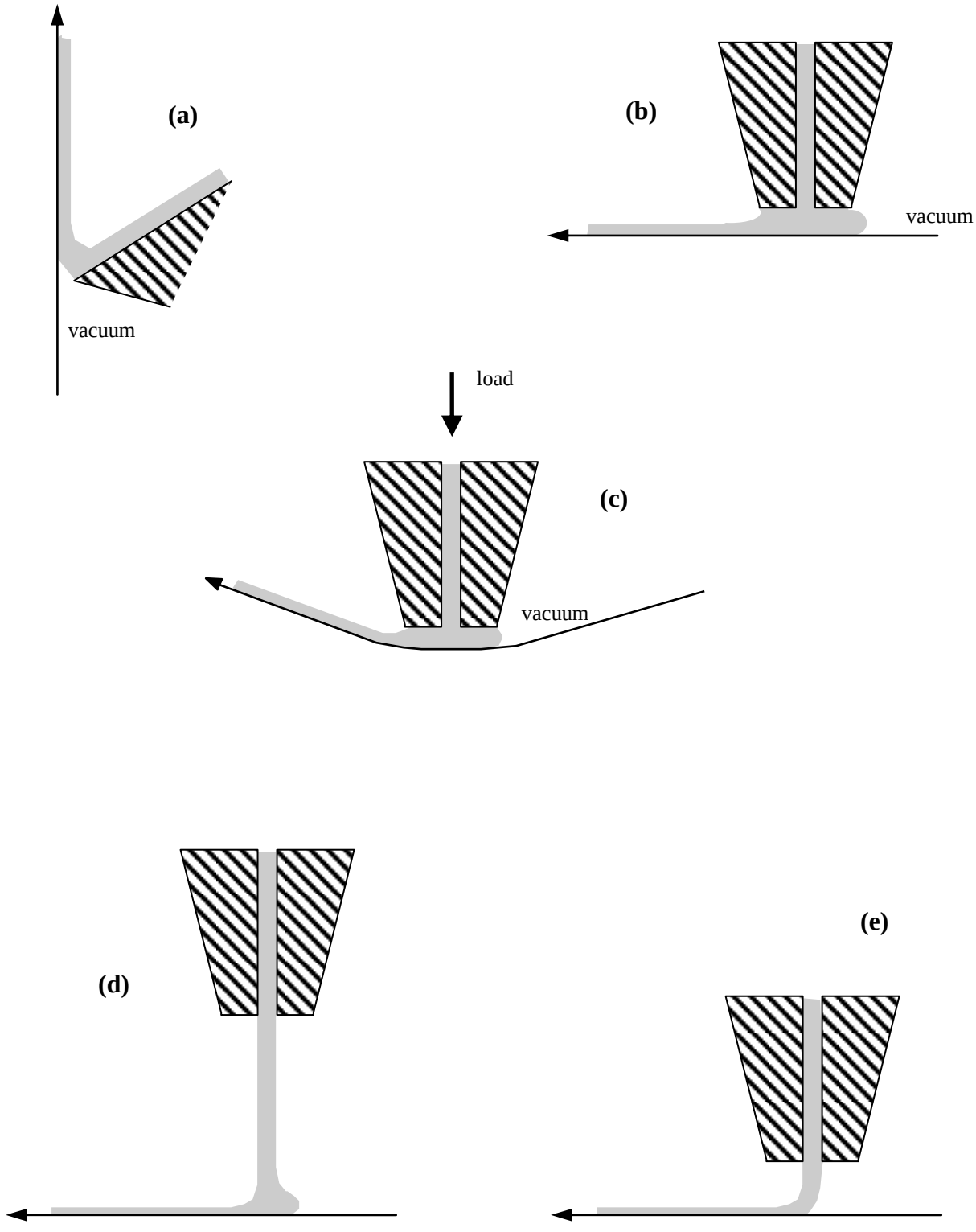

Fig. 16 : Premetered coating processes. (a) slide coating ; (b) slot coating ; (c) die coating ; (d) curtain coating ; (e) extrusion coating

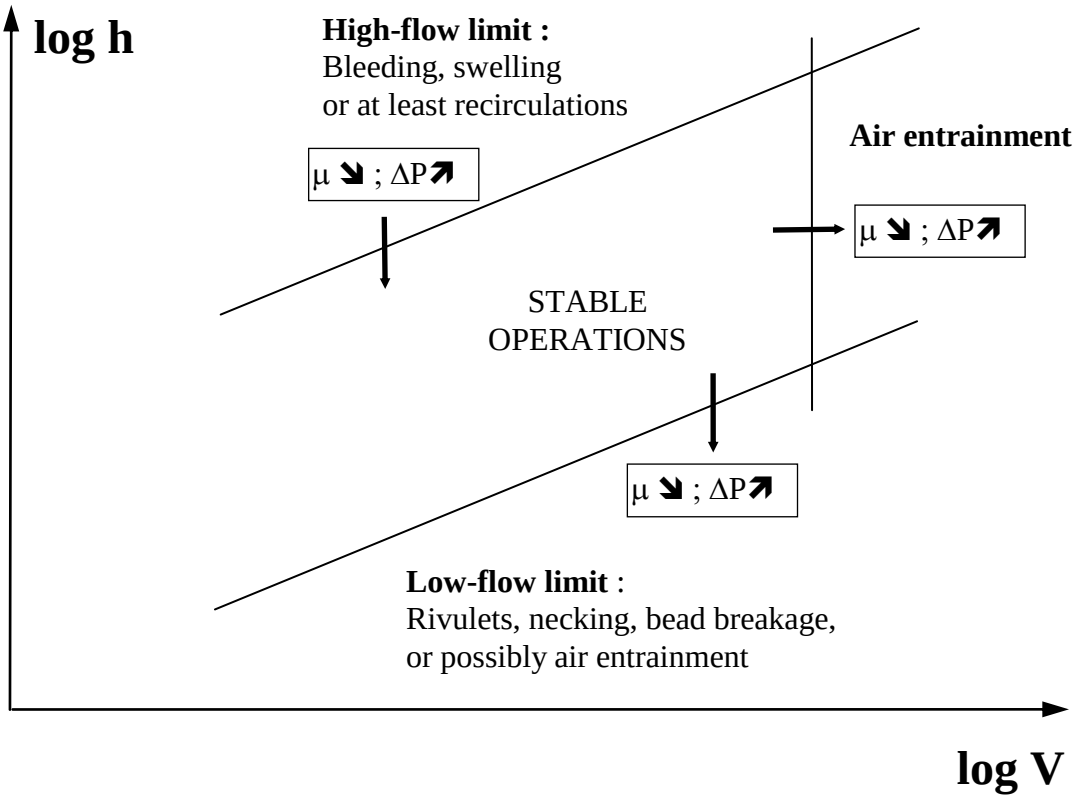

Fig. 17 : Schematic coating window in slide coating

Fig. 18 : Low-flow and air entrainment limits of coatability of a slide coater as measured for various liquids by Gutoff and Kendrick (1987) with 500 Pa bead vacuum.

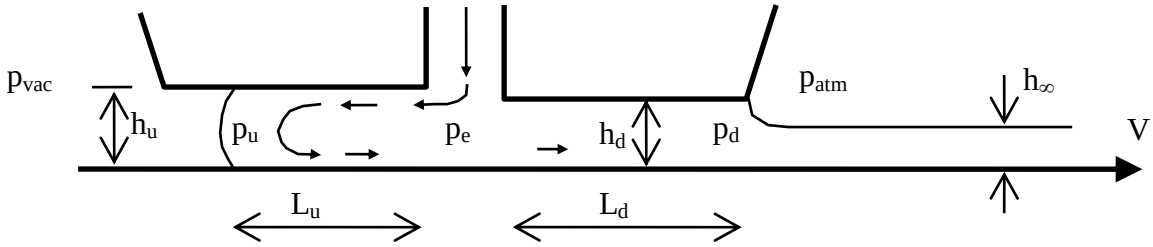

Fig. 19 : Definition sketch of a slot coater

Fig. 20 : Example of a coating window in slot coating (after Scriven & Suszynski, 1994).

Fig. 21 : Example of a coating window showing the low-flow limit of coatability of a slot coater (after Lee *et al.*, 1992).

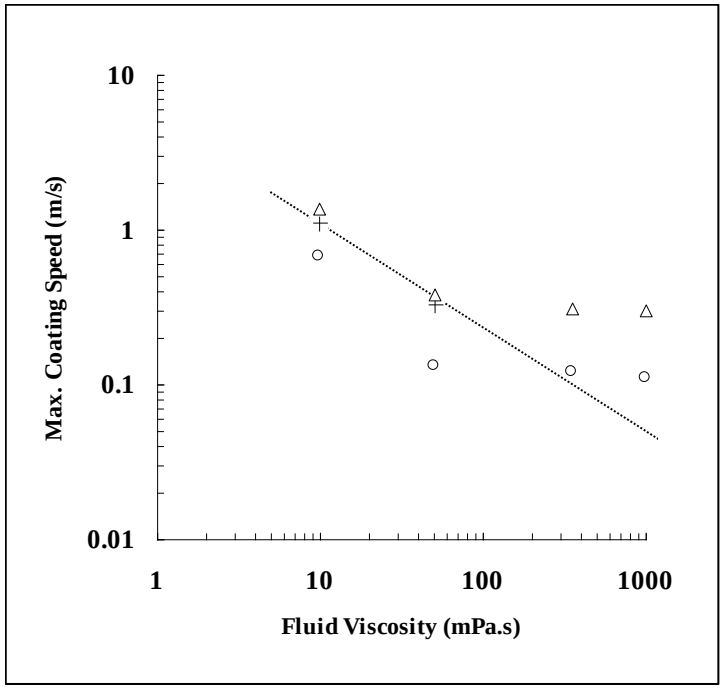

Fig. 22 : Maximum coating speeds in slot coating (data of Lee *et al.*, 1992). Slot gap 1 mm (o), 0.5 mm (+) and 0.2 mm (Δ). --------- : air entrainment velocities in plunging tape experiments, after Gutoff and Kendrick (1982), Eq. [2].

Fig. 23 : Effect of polymer additives concentration on the maximum coating speed in slot coating (after Ning *et al.*, 1996).

Fig. 24 : Schematic coating window in curtain coating (after Blake *et al.*, 1994)

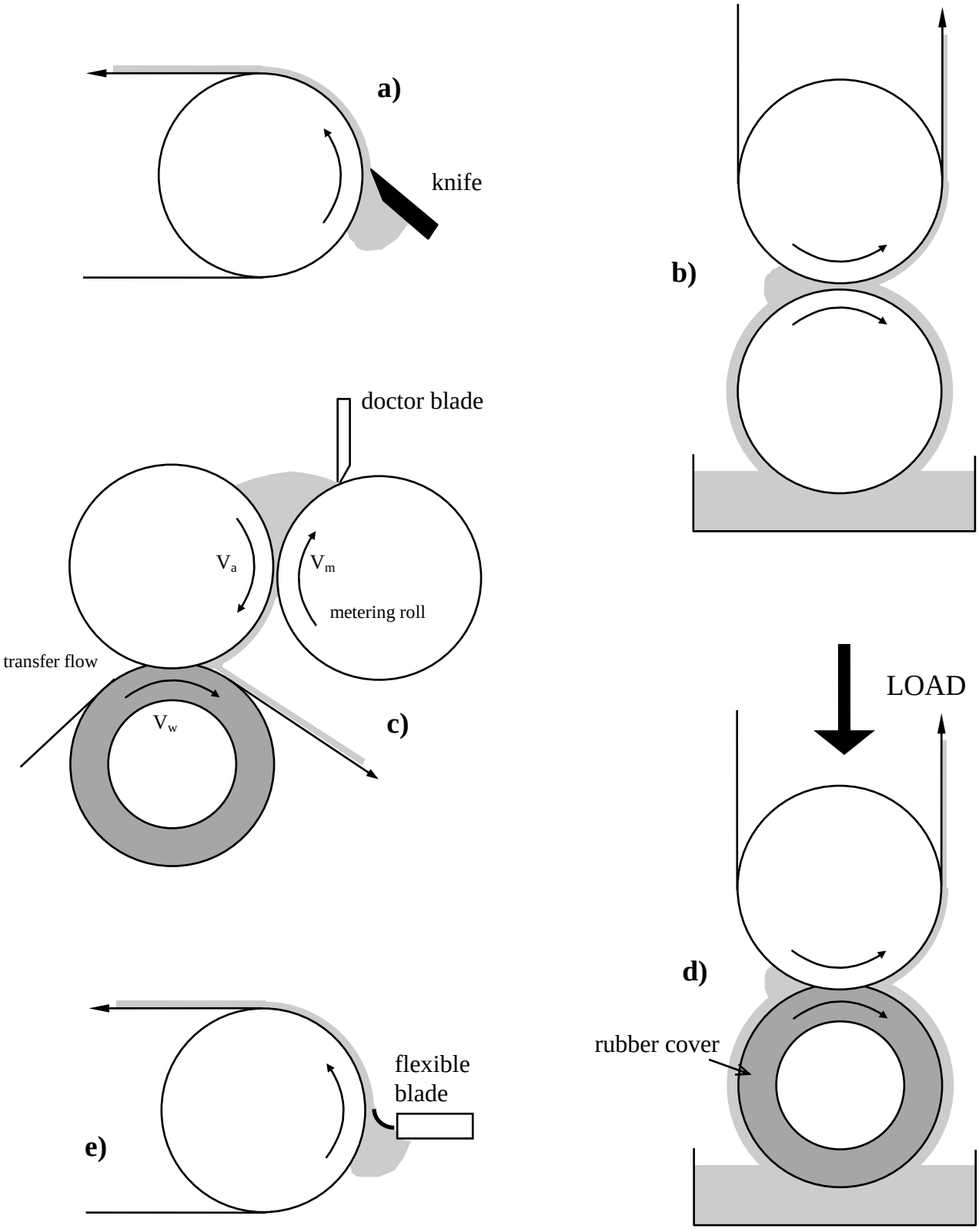

Fig. 6 : Self-metered coating processes. a) knife coating b) forward roll coating c) reverse roll metering with kiss coating transfer d) deformable roll coating e) flexible blade coating

Fig. 7 : Schematic drawing of a perturbation to the film-splitting meniscus in forward roll coating, from which an approximate stability criterion, Eq. [5], can be derived

Fig. 8 : Film-splitting of power-law, shear-thinning liquids in forward roll coating (after Coyle *et al.*, 1987). The Newtonian case corresponds to $n = 1$.

Fig. 9 : Critical capillary number for the onset of ribbing in forward roll coating as a function of gap over radius ratio (after Coyle, 1997).

Fig. 10 : Use of a string in contact with the film-splitting meniscus to eliminate ribbing

Fig. 11 : Metered film thickness in reverse roll coating with Newtonian liquids. Comparison between experiments (dotted lines) and theories (after Coyle *et al.*, 1990b).

Fig. 12 : Effect of polyacrylamide additives on the metered film thickness in reverse roll coating (after Coyle *et al.*, 1990c).

Fig. 13 : Examples of coating windows in reverse roll coating (after Coyle *et al.*, 1990b)

Fig. 14 : Mechanism of cascade instability in reverse roll coating

Fig. 15 : Effects of load, viscosity and speed on the coating thickness in deformable roll coating (after Cohu and Magnin, 1997). E ≈ 3.6 MPa. "Thick" rubber cover (25 mm).

Fig. 25 : Film thicknesses (in units of half-gap width) in reverse meniscus coating (after Richardson *et al.*, 1996).

Fig. 26 : Schematic of the bead in forward meniscus coating.

Fig. 27 : Gravure roller geometries

Fig. 28 : Variation of film thickness with Reynolds number (definied with the substrate speed) in reverse gravure coating (after Benkreira and Patel, 1993).

Fig. 29 : Film thickness in direct forward gravure coating as a function of the average capillary number and the speed ratio $S = V_g / V_s$ (after Benkreira and Cohu, 1997).

Fig. 30 : Typical coating windows in forward, unloaded direct gravure coating (after Benkreira *et al.*, 1996).

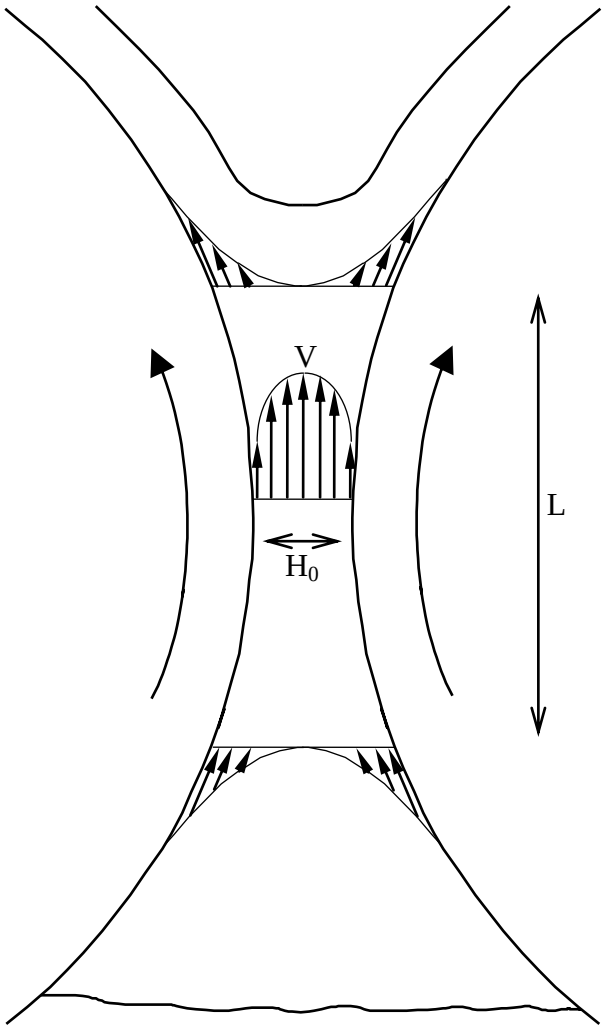

Fig. 1 : Schematic description of the flow kinematics in a roll coating flow